

Deep Residual Axial Networks

Nazmul Shahadat, Anthony S. Maida
 University of Louisiana at Lafayette
 Lafayette LA 70504, USA
 nazmul.ruet@gmail.com, maida@louisiana.edu

Abstract

While residual networks (ResNets) demonstrate outstanding performance on computer vision tasks, their computational cost still remains high. Here, we focus on reducing this cost by proposing a new network architecture, axial ResNet, which replaces spatial 2D convolution operations with two consecutive 1D convolution operations. Convergence of very deep axial ResNets has faced degradation problems which prevent the networks from performing efficiently. To mitigate this, we apply a residual connection to each 1D convolutional operation and propose our final novel architecture namely residual axial networks (RANs). Extensive benchmark evaluation shows that RANs outperform with about 49% fewer parameters than ResNets on CIFAR benchmarks, SVHN, and Tiny ImageNet image classification datasets. Moreover, our proposed RANs show significant improvement in validation performance in comparison to the wide ResNets on CIFAR benchmarks and the deep recursive residual networks on image super resolution dataset.

1. Introduction

Deep convolutional neural network (CNN) based architectures, specifically ResNets [11], have achieved significant success for image processing tasks, including classification [10, 11, 21], object detection [6, 22] and image super-resolution [17, 18, 28]. The performance of deep ResNets and wide ResNets has improved in recent years. Along with the increasing depth or widening of ResNets, the computational cost of the networks also rises. Moreover, training these deeper or wider networks has faced exploding or vanishing gradient and degradation problems. Different initialization, optimization, and normalization techniques [9, 10, 16, 25, 27, 30], skip connections [10], and transfer learning [5] have been used to mitigate these problems. The rising computational cost and/or trainable parameter is still unexplored which is the main purpose of this paper.

However, the computational cost of these deeper and wider ResNets has not been analyzed yet. Deep or wide ResNets gain popularity and impressive performance due to their simple but effective architectures [4, 8, 14, 31, 33]. Deep ResNets can be factored as ensembles of shallow networks [1] and represent functions more efficiently for complex tasks than shallow networks [2]. However, constructing deeper ResNets is not as simple as adding more residual layers. The design of deeper ResNets demands better optimization and initialization schemes, and proper use of identity connections. Deeper ResNets have great success in image classification and object detection tasks [10, 11]. However, the computational cost increases linearly with the number of layers [12].

Wide ResNets use a shallow network with wide (high channel count) architecture to attain better performance than the deeper networks [4, 31, 33]. For example, [33] represented their wide residual network as WRN- n - k where n is the number of convolutional layers and k represents the widening factor. They have shown that their WRN-28-10, wide ResNet that adopts 28 convolutional layers with $k = 10$ widening factor, outperforms the deep ResNet-1001 network (1001 layers). However, the computational cost is quadratic with a widening factor of k .

This work revisits the designs of deep and wide ResNets to boost their performance further, reduce the above-mentioned high computational costs, and improve the model inference speed. To get these, we propose our novel architecture, residual axial networks (RANs), obtained using axial operations, height or width-axis, instead of spatial operations in the residual block. Here, we split 2D spatial (3×3) convolution operation into two consecutive 1D convolution operations. These 1D convolution operations are mapped to the height-axis (3×1) and width-axis (1×3). As axial 1D convolution operations propagate information along one axis at a time, this modification reduces cost significantly. To capture global information, we use these layers in consecutive pairs.

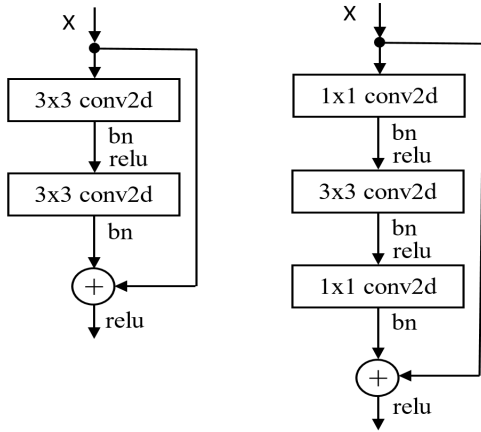


Figure 1. Residual block architectures. “bn” stands for batch normalization. (Left) ResNet basic block and (Right) ResNet bottleneck blocks are depicted.

A simple axial architecture reduces cost but does not improve performance. The reason is that forward information flows across the axial blocks degrades (diminishing feature reuse [15]). To address this, we add residual connections to span the axial blocks. By using both modifications, we made a novel, effective residual axial architecture (RAN). The effectiveness of our proposed model is demonstrated experimentally on four image classification datasets and an image super-resolution dataset. Our assessments are based on parameter counts, FLOPS counts (number of multiply-add operations), latency to process one image after training, and validation accuracy.

2. Background and Related Work

2.1. Convolutional Neural Networks

In a convolutional layer, the core building block is a convolution operation using one kernel W applied to small neighborhoods to find input correlations. For an input image X with height h , width w , and channel count d_{in} , the convolution operation operates on region $(a, b) \in X$ centered at pixel (i, j) with spatial extent k . The output for this operation C_o where $o = (i, j)$ is [26],

$$C_o = \sum_{(a,b) \in \mathcal{N}_{k \times k}(i,j)} W_{i-a,j-b}^{(m)} x_{a,b} \quad (1)$$

where $\mathcal{N}_{k \times k}$ is the neighborhood of pixel (i, j) with spatial extent k , and W is the shared weights to calculate the output for all pixel positions (i, j) .

2.2. Residual Networks

Residual networks (ResNets) are constructed using convolutional layers linked by additive identity connec-

tions [12]. They were introduced to address the problem of vanishing gradients found in standard deep CNNs.

Although, the vanishing gradient problem may be addressed by using normalized inputs and normalization layers which help to make networks till ten layers. In this situation, when more layers were stacked, the network depth increases but accuracy gets saturated and then degrades rapidly. The degradation (of training accuracy) indicates that not all systems are similarly optimized. To address these problems, He et al. proposed residual networks by adding identity mapping among the layers [12]. As a result, the subsequent deeper layers are shared inputs from the learned shallower model. This helps to address all of the problems.

The key architectural feature of ResNets is the residual block with identity mapping to tackle the degradation problem. Two kinds of residual blocks are used in residual networks, the basic block and the bottleneck block, both depicted in Figure 1. Figure 1 (left) is known as the basic architecture of ResNet which is constructed with two $k \times k$ convolution layers where k is the size of the kernel and an identity shortcut connection is added to the end of these two layers to address vanishing gradients. These operations can be expressed mathematically as,

$$y = \mathcal{F}(C_{k_m, k_n}(x, W)) + x \quad (2)$$

where \mathcal{F} , x , y , W , and C_{k_m, k_n} represent residual function, input vector, output vector, weight parameters, and output of two convolution layers with kernels K_m and K_n respectively. Figure 1 (right) is a bottleneck architecture that is constructed using 1×1 , $k \times k$, and 1×1 convolution layers, where the 1×1 layers reduce and then increase the number of channels, and the 3×3 layer performs feature extraction. The identity shortcuts (explained in equation 3) are very important for this block as it leads to more efficient designs [11]. These can be expressed mathematically as,

$$y = \mathcal{F}(C_{k_1, k_m, k_1}(x, W)) + x \quad (3)$$

where \mathcal{F} , x , y , W , and C_{k_1, k_m, k_1} represent residual function, input vector, output vector, weight parameters, and output of three convolution layers with kernels 1×1 , $K_m \times K_m$ and 1×1 respectively. Its performance surpasses the learning speed, number of learning parameters, way of layer-wise representation, difficult optimization property, and memory mechanisms.

2.3. Wide Residual Networks

Wide ResNets [4, 33] use fewer layers compared to standard ResNets but use high channel counts (wide architectures) which compensate for the shallower architecture. The comparison between shallow and deep networks has been revealed in circuit complexity theory

where shallow circuits require more components than the deeper circuit. Inspired by this observation, [11] proposed deeper networks with thinner architecture where a gradient goes through the layers. But the problem such networks face is that the residual block weights do not flow through the network layers. For this, the network may be forced to avoid learning during training. To address these issues, [33] proposed shallow but wide network architectures and showed that widening the residual blocks improves the performance of residual networks compared to increasing their depth. For example, a 16-layer wide ResNet has similar accuracy performance to a 1000-layer thinner network.

2.4. Recursive Residual Networks

Image super-resolution (SR) is the process of generating a high-resolution (HR) image from a low-resolution (LR) image. It is also known as single image super-resolution (SISR). A list of convolution-based models has shown promising results on SISR [7, 17, 18, 28]. These 2D convolutional networks learn a nonlinear mapping from an LR to an HR image in an end-to-end manner. Convolution-based recursive neural networks have been used on SISR, where recursive networks learn detailed and structured information about an image. As image SR requires more image details, pooling is not used in deep models for SISR. Convolution-based SR [7] has shown that the convolution-based LR-HR mapping significantly improves performance for classical shallow methods. Kim et al., introduce two deep CNNs for SR by stacking weight layers [17, 18]. Among them, [18] uses a chain structure recursive layer along with skip-connections to control the model parameters and improve the performance. Deep SR models [17, 18, 23] demand large parameter counts and more storage.

To address these issues, deep recursive residual networks (DRRNs) were proposed as a very deep network structure, which achieves better performance with fewer parameters [28]. It includes both local and global residual learning, where global residual learning (GRL) is being used in the identity branch to estimate the residual image from the input and output of the network. GRL might face degradation problems for deeper networks. To handle this problem, local residual learning (LRL) has been used which carries rich image details to deeper layers and helps gradient flow. The DRRN also used recursive learning of residual units to keep the model more compact. Several recursive blocks (B) has been stacked, followed by a CNN layer which is used to reconstruct the residual between the LR and HR images. Each of these residual blocks decomposed into a number of residual units (U). The number of recursive block B , and the number of residual units U are responsible

for defining network depth. The depth of DRRN d is calculated as,

$$d = (1 + 2 \times U) \times B + 1 \quad (4)$$

Recursive block definition, DRRN formulation, and the loss function of DRRN are defined in [28].

3. Proposed Residual Axial Networks

The convolution-based residual basic and bottleneck blocks [11, 12] have demonstrated significant performance with the help of several state-of-the-art architectures like, ResNets [11], wide ResNets [31], scaling wide ResNets [33], and deep recursive residual networks (DRRNs) [28] on image classification and image super-resolution datasets. Although the bottleneck residual block makes the networks thinner still the basic and bottleneck blocks are not cost-effective and/or parameter efficient. The 2D convolutional operation of these blocks is consuming $\mathcal{O}(N^2)$ resources, where N is the flattened pixels of an image, and $N = hw$ (for a 2D image of height h , width w , and $h = w$). So the cost for a 2D convolutional operation, for an image with height h , and width w , is $\mathcal{O}((hw)^2) = \mathcal{O}(h^2w^2) = \mathcal{O}(h^4)$ [13, 29]. To reduce this impractical computational cost, we are proposing a novel architectural design, residual axial networks (RANs).

Due to high computational expenses, we replace all spatial 2D convolution operations (conv2D) of the residual basic blocks, and the only spatial 2D convolution operation of the residual bottleneck block by using two 1D convolutional operations. Also, each 1D convolutional operation has a residual connection to reduce vanishing gradients. Although this axial technique was introduced in [13] for auto-regressive transformer models, we propose novel architectures by factorizing 2D convolution into two consecutive 1D convolutions. Figures 2, and 3 show our novel proposed residual blocks.

For each location, $o = (i, j)$, a local input kernel $k \times k$ is extracted from an input image X with height h , width w , and channel count d_{in} to serve convolutional operation. Residual units, used by [12], are defined as,

$$Y_o = R(X_o) + \mathcal{F}(X_o, W_o) \quad (5)$$

where, X_o and Y_o are input and output for the location $o = (i, j)$, $R(X_o)$ is the original input or identity mapping, and \mathcal{F} is the residual function. This residual function is defined using convolutional operation for vision tasks. The structure of this residual function depends on the residual block, we use. Two spatial 2D convolutional operations are used for residual basic block, and a spatial (kernel $k > 1$) 2D convolution operation is used in between two convolutional operations (kernel $k = 1$) for

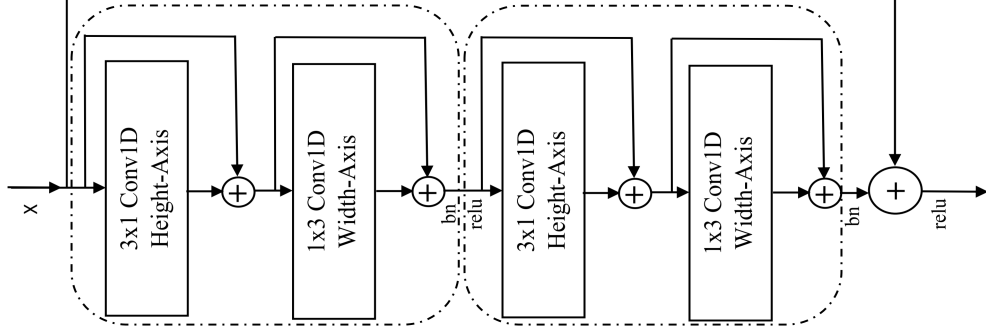


Figure 2. RAN basic block used in our proposed networks. “bn” stands for batch normalization.

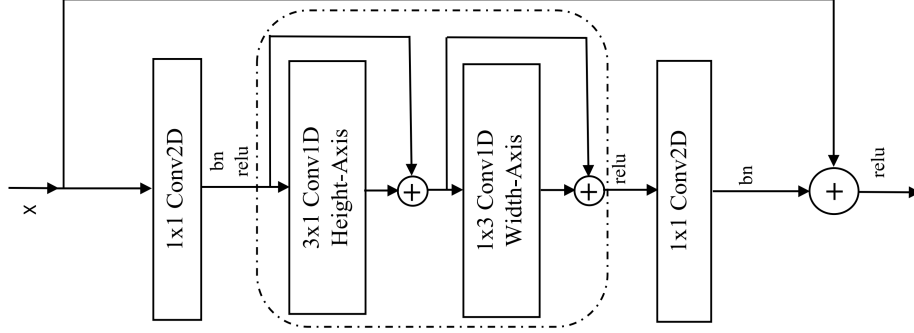


Figure 3. RAN bottleneck block used in our proposed networks. “bn” stands for batch normalization.

bottleneck block. These spatial 2D convolutional operations for kernel $k > 1$ and $o = (i, j)$ can be defined as [26],

$$C_o = \sum_{(a,b) \in \mathcal{N}_{k \times k}(o)} W_{i-a, j-b}, x_{a,b} \quad (6)$$

where, $\mathcal{N}_k \in \mathbb{R}^{k \times k \times d_{in}}$ is the neighborhood of pixel (i, j) with the spatial square region $k \times k$ and $W \in \mathbb{R}^{k \times k \times d_{out} \times d_{in}}$ is the shared weights that are for calculating output for all pixel positions centered by (i, j) . The computational cost is $\mathcal{O}(hwk^2)$ which is high.

To reduce this computation cost and make parameter efficient architecture, we propose to adopt the axial concept and replace 2D convolution using two 1D convolutions with residual connections. These two 1D convolutions are performing convolution along the height axis and the width axis. The 1D convolution along the height axis is defined as follows.

$$C_h = \sum_{(a,b) \in \mathcal{N}_{k \times 1}(i,j)} W_{i-a, j-b}, x_{a,b} \quad (7)$$

where, $\mathcal{N}_k \in \mathbb{R}^{k \times 1 \times d_{in}}$ is the neighborhood of pixel (i, j) with spatial extent $k \times 1$ and $W \in \mathbb{R}^{k \times 1 \times d_{out} \times d_{in}}$ is the shared weights that are for calculating output for all pixel positions (i, j) . And, for width axis is as fol-

lows.

$$C_w = \sum_{(a,b) \in \mathcal{N}_{1 \times k}(i,j)} W_{i-a, j-b}, x_{a,b} \quad (8)$$

where, $\mathcal{N}_k \in \mathbb{R}^{1 \times k \times d_{in}}$ is the neighborhood of pixel (i, j) with spatial extent $1 \times k$ and $W \in \mathbb{R}^{1 \times k \times d_{out} \times d_{in}}$ is the shared weights that are for calculating output for all pixel positions (i, j) .

To construct our basic and bottleneck blocks, we replace each 2D convolution layer from the original residual blocks with a pair of consecutive 1D convolution layers. When we did this but omitted a residual connection, the network faced the vanishing gradient problem. To handle this, we added a residual connection along each 1D convolution operation. Each 2D convolution in Equation 6 is equivalent to our proposed method defined as,

$$Y_h = C_h(W_h, X_o) + X_o \quad (9)$$

$$Y_o = C_w(W_w, Y_h) + Y_h \quad (10)$$

where, C_h , and C_w are the height and width outputs of Equations 7 and 8, respectively, W_h , and W_w is the convolutional weights for height, and width axis 1D convolutional operations, respectively. Equation 10 describes the residual basic and bottleneck blocks. As two 1D operations equal one 2D operation, the use of these two

layers does not increase the layer count. The RAN basic and bottleneck blocks are shown in Figures 2 and 3. These blocks are used to construct our proposed residual axial networks (RANs). The output Y_o from Equation 10 is applied to other 2D convolution-based networks, for example, wide residual networks (to make our proposed wide RANs) and deep recursive residual networks (to make RARNets), to check the effectiveness of our proposed method.

4. Experimental Analysis

We present experimental results on four image classification datasets and one image super-resolution dataset. Our experiments evaluate the proposed residual axial networks, the original ResNets, the wide ResNets, wide RANs, the deep recursive residual networks (DRRN), and RARNets. We compare our proposed network’s performance with the corresponding original ResNets, as these original networks used 2D spatial convolutional layers. Our comparisons use parameter counts, FLOPS, latency, and validation performance.

4.1. Method: Residual Networks

To explore scalability, we compare our proposed RANs and baseline models on four datasets: CIFAR-10 and CIFAR-100 benchmarks [19], Street View House Number (SVHN) [24], and Tiny ImageNet datasets [20]. The CIFAR benchmarks have 10 and 100 distinct classes, and 60,000 color images (split into 50,000 training and 10,000 testing images) of size 32×32 . We perform data normalization using per-channel mean and standard deviation. In preprocessing, we do a horizontal flip and randomly crop after padding with four pixels on each side of the image. The SVHN and Tiny ImageNet datasets contain 600,000 images of size 32×32 with ten classes and 110,000 images of 200 distinct classes downsized to 64×64 colored images, respectively. Our only preprocessing is mean/std normalization for both datasets.

All the models (baselines and proposed RANs) were trained using similar architectures (same hyperparameters and the same number of output channels). As our main concern was to reduce the parameter counts of the bottleneck residual block, we implemented all network architecture, baselines, and proposed, using only bottleneck blocks. The numbers of output channels of bottleneck groups are 120, 240, 480, and 960 for all networks. This experiment analyzes 26, 35, 50, 101, and 152-layer architectures with the bottleneck block multipliers “[1, 2, 4, 1]”, “[2, 3, 4, 2]”, “[3, 4, 6, 3]”, “[3, 4, 23, 3]”, and “[3, 8, 36, 3]”, respectively. All models were run using the stochastic gradient descent optimizer, and using linearly warmed-up learning for 10 epochs from zero

to 0.1 and then used cosine learning scheduling from epochs 11 to 150. All models were trained using batch sizes of 128 for all datasets, we used except the 101, and 152-layer architectures of the Tiny ImageNet dataset. We used a batch size of 64 for these two architectures on Tiny ImageNet.

4.2. Results: Residual Networks

Table 1 summarizes the classification results of the original ResNets and our proposed RANs on the four datasets. We tested shallow and deeper networks by implementing 26, 35, 50, 101, and 152-layer architectures. These architectures compare performance to check the effectiveness of our proposed methods for shallow and deep networks. Our proposed method is compared with original ResNets in terms of parameter count, FLOPS count (number of multiply-add operations), inference time or latency (time used to test one image after training), and the percentage accuracy of validation results on the four datasets.

The 26, 35, 50, 101, and 152-layer architectures reduce by 48.6%, 46.5%, 44.8%, 43.2%, and 42.6% the trainable parameters respectively needed in comparison to the baseline networks. In addition to parameter reduction, our proposed method requires 15 to 36 percent fewer FLOPS for all analyzed architectures. Also, the validation performance improvement is significantly noticeable for all datasets. The latency to process one image after training our proposed models is comparatively high as the RANs use two convolution layers sequentially. It is also shown that the deeper networks perform better than the shallow networks and it has demonstrated “the deeper, the better” in classification.

4.3. Method: Wide Residual Networks

The previous experiment did not assess wide ResNets. To assess the widening factor on our proposed RANs, we increase the width of our RANs by factorizing the number of output channels for shallow networks like [33]. Like the original wide residual networks (WRNs) [33], we analyzed our proposed 26-layer bottleneck block of RANs with a widening factor, $k = 2, 4, 6, 8,$ and 10. We multiplied the number of output channels of RANs with k to obtain wide RANs. We performed training with the same optimizer and hyperparameters used in 4.1.

4.4. Results: Wide Residual Networks

Table 1 shows “the deeper the better” in vision classification for our proposed methods. To compare our proposed RANs with the original wide ResNets (WRNs), we analyze our proposed method for different widening factors. Table 2 shows an overall comparison among the original WRN-28-10 (28-layers with a widening factor

Dataset	Model Name	Layers	Params	FLOPs	Latency	Accuracy
CIFAR-10	ResNet [11]	26	40.9M	0.66G	0.66ms	94.68
	RAN (Ours)		21M	0.56G	0.73ms	96.08
	ResNet [11]	35	57.8M	0.86G	0.82ms	94.95
	RAN (Ours)		30.9M	0.68G	0.91ms	96.15
	ResNet [11]	50	82.5M	1.18G	1.02ms	95.08
	RAN (Ours)		45.5M	0.87G	1.17ms	96.25
	ResNet [11]	101	149.2M	2.29G	1.68ms	95.36
	RAN (Ours)		84.7M	1.52G	1.86ms	96.27
ResNet [11]	152	204.1M	3.41G	2.39ms	95.36	
RAN (Ours)		117.1M	2.18G	2.55ms	96.37	
CIFAR-100	ResNet [11]	26	41.2M	0.66G	0.66ms	78.21
	RAN (Ours)		21.1M	0.56G	0.74ms	79.66
	ResNet [11]	35	58.1M	0.86G	0.80ms	78.72
	RAN (Ours)		31.1M	0.68G	0.91ms	80.38
	ResNet [11]	50	82.9M	1.18G	1.11ms	78.95
	RAN (Ours)		45.7M	0.87G	1.17ms	80.84
	ResNet [11]	101	149.5M	2.29G	1.72ms	78.80
	RAN (Ours)		84.9M	1.52G	1.86ms	80.88
ResNet [11]	152	204.5M	3.41G	2.36ms	79.85	
RAN (Ours)		117.2M	2.18G	2.55ms	80.94	
SVHN	ResNet [11]	26	40.9M	0.66G	0.64ms	96.04
	RAN (Ours)		21M	0.56G	0.73ms	97.60
	ResNet [11]	35	57.8M	0.86G	0.79ms	95.74
	RAN (Ours)		30.9M	0.68G	0.90ms	97.50
	ResNet [11]	50	82.5M	1.18G	1.05ms	95.76
	RAN (Ours)		45.5M	0.87G	1.11ms	97.32
	ResNet [11]	101	149.2M	2.29G	1.64ms	96.29
	RAN (Ours)		84.7M	1.52G	1.80ms	97.29
ResNet [11]	152	204.1M	3.41G	2.28ms	96.35	
RAN (Ours)		117.1M	2.18G	2.5ms	97.38	
ImageNet-Tiny	ResNet [11]	26	41.6M	0.66G	2.31ms	57.21
	RAN (Ours)		21.3M	0.56G	2.58ms	62.28
	ResNet [11]	35	58.5M	0.86G	2.85ms	57.80
	RAN (Ours)		31.3M	0.68G	3.0ms	59.31
	ResNet [11]	50	82.6M	1.18G	3.75ms	59.06
	RAN (Ours)		45.8M	0.87G	4.02ms	62.40
	ResNet [11]	101	149.3M	2.29G	6.86ms	60.62
	RAN (Ours)		85.1M	1.52G	7.19ms	64.18
ResNet [11]	152	204.2M	3.41G	9.29ms	61.57	
RAN (Ours)		117.4M	2.18G	9.72ms	66.16	

Table 1. Image classification performance on the CIFAR benchmarks, SVHN, and Tiny ImageNet datasets for 26, 35, 50, 101, and 152-layer architectures.

of 10), and our proposed 26-layer networks with different widening factors ($k = 2, 4, 6, 8,$ and 10). Our proposed wide RANs show significant accuracy improvement over the original WRN-28-10. This table also demonstrates “the wider the better” for our proposed wide RANs.

4.5. Method: Recursive Networks

This experiment compares the cost and performance of our novel RARnet with the DRRN on the super-resolution tasks. The RARnet is built by replacing the residual unit U with a RAN layer described in Equation 10. These modifications form a new architecture, recursive axial residual network (RARNet) whose depth d is

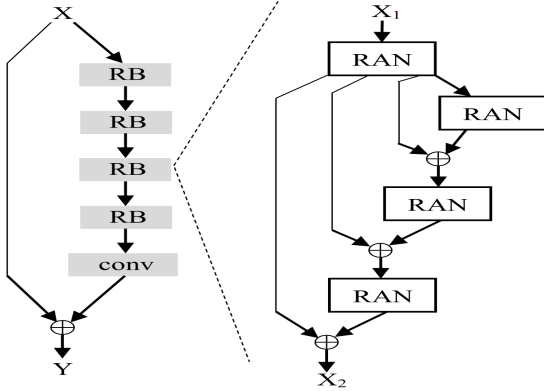


Figure 4. Recursive axial residual network (RARNet) architecture with $B = 4$ and $U = 3$. Here, “RB” layer, and RAN refer to a recursive block, and residual axial block, respectively.

defined as,

$$d = (1 + U_{RAN}) \times B + 1 \quad (11)$$

As two 1D layers are equivalent to one 2D layer and we replace each residual unit by a RAN unit (see Equation 10). Hence, we rewrite Equation 4 to Equation 11 by removing the multiplier for the residual unit. The proposed RARNet with four RB blocks is shown on the left in Figure 4. An RB block is expanded on the right.

We trained our proposed RARNet using 291 images dataset [32] and tested using the Set5 dataset [3]. We also use different scales ($\times 2$, $\times 3$, and $\times 4$) in training and testing images. We used similar data augmentation, training hyperparameters, and implementation details like [28].

4.6. Results: Recursive Networks

Table 3 shows the Peak Signal-to-Noise Ratio (PSNR) results of several CNN models including DRRN, and our proposed RARNet on the Set5 dataset. The comparison between DRRN and RARNet is our main focus as it directly indicates the effectiveness of using our proposed RAN block. DRRN19 and DRRN125 are constructed using $B = 1, U = 9$, and $B = 1, U = 25$, respectively. For fair comparison, we also construct similar architecture like RARNet19 ($B = 1, U_{RAN} = 9$) and RARNet125 ($B = 1, U_{RAN} = 25$). Our proposed models outperform all CNN models in Table 3 on the Set5 dataset and for all scaling factors. As we are trying to propose a parameter-efficient architecture, parameter comparison is very essential along with the testing performance. Our proposed model for $B = 1$, and $U_{RAN} = 9$ takes 213,254 parameters compared to 297,216 parameters of DRRN ($B = 1$, and $U = 9$). RARNet, which is constructed using RAN blocks, reduces by 28.2% the trainable parameters compared to

Dataset	Model Name	Accuracy
CIFAR-10	WRN-28-10 [33]	94.68
	RAN-26-2 (Ours)	96.32
	RAN-26-4 (Ours)	96.68
	RAN-26-6 (Ours)	96.77
	RAN-26-8 (Ours)	96.83
	RAN-26-10 (Ours)	96.87
CIFAR-100	WRN-28-10 [33]	79.57
	RAN-26-2 (Ours)	83.54
	RAN-26-4 (Ours)	83.75
	RAN-26-6 (Ours)	83.78
	RAN-26-8 (Ours)	83.82
	RAN-26-10 (Ours)	83.92

Table 2. Image classification performance comparison on the CIFAR benchmarks for 26-layer RAN architectures with different widening factors.

the DRRN.

5. Discussion and Conclusions

This work introduces a new residual block that can be used as a replacement for the ResNet basic and bottleneck blocks. This RAN block replaced the 2D convolution from the original ResNet blocks with two sequential 1D convolutions along with a residual connection. These modifications help to reduce trainable parameters as well as improve validation performance on vision classification. But the latency of our proposed model is comparatively high. The proposed model’s performance and parameter reduction outweigh this latency time limitation. We also checked this proposed block for widened ResNets and showed that the wide RANs obtain better accuracy performance than the WRNs. We also checked the effectiveness of RANs on the SISR task. Specifically, we applied our proposed RAN block on an image restoration dataset and found that our proposed recursive axial ResNets (RARNets) improve image resolution and reduce trainable parameters more than the other CNN-based super-resolution models. Extensive experiments and analysis show that RANs can be deep, and wide and these are parameter-efficient and superior models for image classification and SISR. We have shown that our proposed model is a viable replacement for ResNets on the tasks that were tested. Further work is required to determine the range of applications for which RANs may offer advantages.

References

- [1] Serge Belongie, Michael Wilber, and Andreas Veit. Residual networks behave like ensembles of relatively shallow networks. 2016. 1

Dataset	Scale	SRCNN [7]	VDSR [17]	DRCN [18]	DRRN19	DRRN125	RARNet19	RARNet25
Set5	x2	36.66	37.53	37.63	37.66	37.74	37.73	37.84
	x3	32.75	33.66	33.82	33.93	34.03	33.99	34.11
	x4	30.48	31.35	31.53	31.58	31.68	31.63	31.84

Table 3. Benchmark testing PSNR results for scaling factors $\times 2$, $\times 3$, and $\times 4$ on Set5 dataset.

- [2] Yoshua Bengio, Aaron Courville, and Pascal Vincent. Representation learning: A review and new perspectives. *IEEE transactions on pattern analysis and machine intelligence*, 35(8):1798–1828, 2013. 1
- [3] Marco Bevilacqua, Aline Roumy, Christine Guillemot, and Marie Line Alberi-Morel. Low-complexity single-image super-resolution based on nonnegative neighbor embedding. 2012. 7
- [4] Liang-Chieh Chen, Huiyu Wang, and Siyuan Qiao. Scaling wide residual networks for panoptic segmentation. *arXiv preprint arXiv:2011.11675*, 2020. 1, 2
- [5] Tianqi Chen, Ian Goodfellow, and Jonathon Shlens. Net2net: Accelerating learning via knowledge transfer. *arXiv preprint arXiv:1511.05641*, 2015. 1
- [6] Jifeng Dai, Yi Li, Kaiming He, and Jian Sun. R-fcn: Object detection via region-based fully convolutional networks. *Advances in neural information processing systems*, 29, 2016. 1
- [7] Chao Dong, Chen Change Loy, Kaiming He, and Xiaoou Tang. Image super-resolution using deep convolutional networks. *IEEE transactions on pattern analysis and machine intelligence*, 38(2):295–307, 2015. 3, 8
- [8] Shang-Hua Gao, Ming-Ming Cheng, Kai Zhao, Xin-Yu Zhang, Ming-Hsuan Yang, and Philip Torr. Res2net: A new multi-scale backbone architecture. *IEEE transactions on pattern analysis and machine intelligence*, 43(2):652–662, 2019. 1
- [9] Xavier Glorot and Yoshua Bengio. Understanding the difficulty of training deep feedforward neural networks. In *Proceedings of the thirteenth international conference on artificial intelligence and statistics*, pages 249–256. JMLR Workshop and Conference Proceedings, 2010. 1
- [10] Kaiming He, Xiangyu Zhang, Shaoqing Ren, and Jian Sun. Delving deep into rectifiers: Surpassing human-level performance on imagenet classification. In *Proceedings of the IEEE international conference on computer vision*, pages 1026–1034, 2015. 1
- [11] Kaiming He, Xiangyu Zhang, Shaoqing Ren, and Jian Sun. Deep residual learning for image recognition. In *Proceedings of the IEEE conference on computer vision and pattern recognition*, pages 770–778, 2016. 1, 2, 3, 6
- [12] Kaiming He, Xiangyu Zhang, Shaoqing Ren, and Jian Sun. Identity mappings in deep residual networks. In *European conference on computer vision*, pages 630–645. Springer, 2016. 1, 2, 3
- [13] Jonathan Ho, Nal Kalchbrenner, Dirk Weissenborn, and Tim Salimans. Axial attention in multidimensional transformers. *arXiv preprint arXiv:1912.12180*, 2019. 3
- [14] Jie Hu, Li Shen, and Gang Sun. Squeeze-and-excitation networks. In *Proceedings of the IEEE conference on computer vision and pattern recognition*, pages 7132–7141, 2018. 1
- [15] Gao Huang, Yu Sun, Zhuang Liu, Daniel Sedra, and Kilian Q. Weinberger. Deep networks with stochastic depth. In Bastian Leibe, Jiri Matas, Nicu Sebe, and Max Welling, editors, *Computer Vision – ECCV 2016*, pages 646–661, Cham, 2016. Springer International Publishing. 2
- [16] Sergey Ioffe and Christian Szegedy. Batch normalization: Accelerating deep network training by reducing internal covariate shift. In *International conference on machine learning*, pages 448–456. PMLR, 2015. 1
- [17] Jiwon Kim, Jung Kwon Lee, and Kyoung Mu Lee. Accurate image super-resolution using very deep convolutional networks. In *Proceedings of the IEEE conference on computer vision and pattern recognition*, pages 1646–1654, 2016. 1, 3, 8
- [18] Jiwon Kim, Jung Kwon Lee, and Kyoung Mu Lee. Deeply-recursive convolutional network for image super-resolution. In *Proceedings of the IEEE conference on computer vision and pattern recognition*, pages 1637–1645, 2016. 1, 3, 8
- [19] Alex Krizhevsky, Geoffrey Hinton, et al. Learning multiple layers of features from tiny images. 2009. 5
- [20] Ya Le and Xuan S. Yang. Tiny imagenet visual recognition challenge. 2015. 5
- [21] Xiu Li and Zuoying Cui. Deep residual networks for plankton classification. In *OCEANS 2016 MTS/IEEE Monterey*, pages 1–4, 2016. 1
- [22] Tsung-Yi Lin, Piotr Dollár, Ross Girshick, Kaiming He, Bharath Hariharan, and Serge Belongie. Feature pyramid networks for object detection. In *Proceedings of the IEEE conference on computer vision and pattern recognition*, pages 2117–2125, 2017. 1
- [23] Xiaojiao Mao, Chunhua Shen, and Yu-Bin Yang. Image restoration using very deep convolutional encoder-decoder networks with symmetric skip connections. *Advances in neural information processing systems*, 29, 2016. 3
- [24] Yuval Netzer, Tao Wang, Adam Coates, Alessandro Bisacco, Bo Wu, and Andrew Y Ng. Reading digits in natural images with unsupervised feature learning. 2011. 5
- [25] Siyuan Qiao, Huiyu Wang, Chenxi Liu, Wei Shen, and Alan Yuille. Micro-batch training with batch-channel normalization and weight standardization. *arXiv preprint arXiv:1903.10520*, 2019. 1
- [26] Prajit Ramachandran, Niki Parmar, Ashish Vaswani, Irwan Bello, Anselm Levskaya, and Jonathon Shlens. Stand-alone self-attention in vision models. *arXiv preprint arXiv:1906.05909*, 2019. 2, 4

- [27] Ilya Sutskever, James Martens, George Dahl, and Geoffrey Hinton. On the importance of initialization and momentum in deep learning. In *International conference on machine learning*, pages 1139–1147. PMLR, 2013. [1](#)
- [28] Ying Tai, Jian Yang, and Xiaoming Liu. Image super-resolution via deep recursive residual network. In *Proceedings of the IEEE conference on computer vision and pattern recognition*, pages 3147–3155, 2017. [1](#), [3](#), [7](#)
- [29] Huiyu Wang, Yukun Zhu, Bradley Green, Hartwig Adam, Alan Yuille, and Liang-Chieh Chen. Axial-deeplab: Stand-alone axial-attention for panoptic segmentation. In *European Conference on Computer Vision*, pages 108–126. Springer, 2020. [3](#)
- [30] Yuxin Wu and Kaiming He. Group normalization. In *Proceedings of the European conference on computer vision (ECCV)*, pages 3–19, 2018. [1](#)
- [31] Zifeng Wu, Chunhua Shen, and Anton Van Den Hengel. Wider or deeper: Revisiting the resnet model for visual recognition. *Pattern Recognition*, 90:119–133, 2019. [1](#), [3](#)
- [32] Jianchao Yang, John Wright, Thomas S Huang, and Yi Ma. Image super-resolution via sparse representation. *IEEE transactions on image processing*, 19(11):2861–2873, 2010. [7](#)
- [33] Sergey Zagoruyko and Nikos Komodakis. Wide residual networks. *arXiv preprint arXiv:1605.07146*, 2016. [1](#), [2](#), [3](#), [5](#), [7](#)